Inorg. Chem. **2005**, *44*, 8418–8425

Characterization and Comparison of Cm(III) and Eu(III) Complexed with 2,6-Di(5,6-dipropyl-1,2,4-triazin-3-yl)pyridine Using EXAFS, TRFLS, and Quantum-Chemical Methods

Melissa A. Denecke, André Rossberg,† Petra J. Panak, Michael Weigl, Bernd Schimmelpfennig, and Andreas Geist*

Forschungszentrum Karlsruhe GmbH, Institut für Nukleare Entsorgung, P.O. Box 3640, 76021 Karlsruhe, Germany, and Forschungszentrum Rossendorf e.V., Institute of Radiochemistry, P.O. Box 510119, 01314 Dresden, Germany

Received July 13, 2005

The complexation of Cm(III) and Eu(III) with 2,6-di(5,6-dipropyl-1,2,4-triazin-3-yl)pyridine (*n*-C_3H_7–BTP) in nonaqueous organic solution is studied with extended X-ray absorption spectroscopy. Bond lengths are the same in both complexes. Quantum-chemical calculations performed at different levels support this finding. On the other hand, the Cm·(*n*-C_3H_7–BTP)$_3$ complex is formed at much lower ligand-to-metal concentration ratio than the Eu·(*n*-C_3H_7–BTP)$_3$ complex, as shown by time-resolved laser-induced fluorescence spectroscopy. This is in good agreement with *n*-C_3H_7–BTP's high selectivity for trivalent actinides over lanthanides in liquid–liquid extraction.

Introduction

Alkylated 2,6-di(1,2,4-triazin-3-yl)pyridines (BTPs, Scheme 1) are highly effective extractants for the separation of trivalent minor actinides (americium, curium) from lanthanides.[1,2] Numerous extractants of similar structures have been developed over the years,[3−5] but BTPs are the first to be used to effectively perform extractions from aqueous solutions of rather high acidity; americium and curium are extracted from up to 1 M nitric acid. Separation factors for americium or curium versus europium of >100 are found for liquid−liquid extraction.[4]

The separation of trivalent actinides (An(III)) from lanthanides (Ln(III)) is a key step in the partitioning and transmutation (P&T) strategy[6] with the aim of separating long-lived actinides from spent nuclear fuels and transmuting them by nuclear fission into shorter-lived isotopes. This would have a positive impact on the long-term radiotoxicity of high-level nuclear wastes to be stored in a final geological repository.

Scheme 1. 2,6-Di(5,6-dialkyl-1,2,4-triazin-3-yl)pyridines[a]

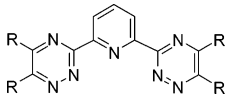

[a] R = CH_3, C_2H_5, *n*-C_3H_7, *i*-C_3H_7, *n*-C_4H_9, *i*-C_4H_9. In this study, R = *n*-C_3H_7.

The task of An(III)−Ln(III) separation is not feasible using common oxygen-donor extractants. Only complexation via soft donors, such as sulfur or nitrogen atoms, for extraction yields the desired selectivity.[7] It is generally accepted that soft donor atoms do not favorably complex hard acceptors such as actinide and lanthanide cations, according to the hard acid−soft base principle. Nevertheless, a more covalent bonding to actinides is considered responsible for the observed selectivity of such soft donors for actinides over lanthanides.[8] To understand this selectivity, as well as to optimize partitioning extractant properties, much interest is

* To whom correspondence should be addressed. E-mail: geist@ine.fzk.de.
† Forschungszentrum Rossendorf e.V., Institute of Radiochemistry.

(1) Kolarik, Z.; Müllich, U.; Gassner, F. *Solvent Extr. Ion Exch.* **1999**, *17* (1), 23−32.
(2) Kolarik, Z.; Müllich, U.; Gassner, F. *Solvent Extr. Ion Exch.* **1999**, *17* (5), 1155−1170.
(3) Madic, C.; Hudson, M. J. *High-level liquid waste partitioning by means of completely incinerable extractants*; EUR 18038; European Commission: Luxembourg, 1998.
(4) Madic, C.; Hudson, M. J.; Liljenzin, J.-O.; Glatz, J. P.; Nannicini, R.; Facchini, A.; Kolarik, Z.; Odoj, R. *New partitioning techniques for minor actinides*; EUR 19149; European Commission: Luxembourg, 2000.
(5) Madic, C.; Testard, F.; Hudson, M. J.; Liljenzin, J.-O.; Christiansen, B.; Ferrando, M.; Facchini, A.; Geist, A.; Modolo, G.; Gonzales-Espartero, A.; De Mendoza, J. *PARTNEW—New solvent extraction processes for minor actinides*; CEA-R-6066; Commissariat à l'Énergie Atomique: France, 2004.
(6) *Actinide and fission product partitioning and transmutation, status and assessment report*; OECD Nuclear Energy Agency: Paris, 1999.
(7) Nash, K. L. *Solvent Extr. Ion Exch.* **1993**, *11* (4), 729−768.

10.1021/ic0511726 CCC: $30.25 © 2005 American Chemical Society
Published on Web 10/07/2005

devoted to finding a relationship between selectivity or extraction performance and structural or electronic properties of An(III) and Ln(III) complexed with partitioning agents such as BTP.

BTPs are able to extract trivalent actinide or lanthanide nitrates from nitrate or nitric acid solutions, according to

$$M^{3+}_{aq} + 3NO_3^-{}_{aq} + 3BTP_{org} \rightleftarrows M\cdot(BTP)_3\cdot(NO_3)_{3\,org} \quad (1)$$

$$M^{3+}_{aq} + 3NO_3^-{}_{aq} + HNO_{3aq} + 3BTP_{org} \rightleftarrows M\cdot(BTP)_3\cdot(NO_3)_3\cdot HNO_{3\,org} \quad (2)$$

That An(III) and Ln(III) cations are complexed by three BTP ligands at relatively high ligand concentration is known from the slope analysis of liquid−liquid extraction data.[2] Slope analysis, however, does not yield information on the complex geometry or structure (i.e., the number of donor−metal bonds form, the number of ligand molecules in the inner coordination sphere, and the length of the bonds).

Drew et al.[9] determined the structure of Ln·(*n*-C_3H_7−BTP)$_3$ crystals using X-ray diffraction, confirming that the complex is composed of three ligands directly bonded to the metal ion. In these crystal structures, BTPs act as tridentate ligands, coordinating via N_{py} (the pyridine N atom) and N_{tz} (the triazinyl N atoms in 2-position, see Scheme 1).

U(III) and Ce(III) complexed with BTPs were compared by Iveson et al.[10] using ^{1}H NMR and X-ray crystallography. By NMR titration, the formation of a U·(CH_3−BTP)$_3$ complex was identified, even when an excess amount of metal cation was present. In contrast, depending on the ratio of metal cation to CH_3−BTP ligand, Ce·(CH_3−BTP)$_2$ and Ce·(CH_3−BTP)$_3$ were found. These observations may be considered as an indication of the higher affinity of BTPs for trivalent actinides. X-ray crystallography identified similar structures for both U·(*n*-C_3H_7−BTP)$_3$ and Ce·(*n*-C_3H_7−BTP)$_3$, namely nonacoordinated metal ions in a slightly distorted tricapped trigonal-prism coordination geometry. These structures are in good agreement with those from ref 9. Interestingly, the U−N bond lengths were found to be 0.06−0.09 Å shorter than the Ce−N bond lengths, although the radii of these two metal cations are quite similar.[11] The authors concluded that the shorter bond lengths in the U(III) complex reflect some degree of covalency in the U−N bond. This work was later extended[12] to include crystal structures of La, Ce, Nd, and U complexed with 2,2′:6′,2″-terpyridine (terpy) and La·(CH_3−BTP)$_3$ and Ce·(CH_3−BTP)$_3$ complexes. In that study, U−N bonds were again reported to be significantly shorter than both the La−N and Ce−N bonds, although the ionic radius of U(III) lies intermediate between those of La(III) and Ce(III). Furthermore, BTP complexes of U(III) and Ln(III) show larger differences in U−N and Ln−N bond lengths, compared to those of their terpy complex counterparts. This observation likely correlates with the higher selectivity of BTP over that of terpy.

Similar differences in U−N and Ce−N bond lengths were observed by Mazzanti et al. and Karmazin et al. in XRD studies of tris[(2-pyrazinyl)methyl]amine (tpza), *N*,*N*,*N*′,*N*′-tetrakis(2-pyrazinylmethyl)*trans*-1,2-cyclohexanediamine (tpzcn), and *N*,*N*,*N*′,*N*′-tetrakis(2-pyrazinylmethyl)trimethylenediamine (tpztn) complexes.[13,14] The tripodal ligand, tpza, and the tetrapodal ligand, *N*,*N*,*N*′,*N*′-tetrakis(2-pyrazinylmethyl)ethylenediamine (tpzen), exhibit high selectivity for Am(III) over Eu(III).[15,16]

Electrospray mass spectrometry was used by Colette et al.[17] to determine composition and stability of Eu·(R−BTP)$_n$ (n = 1−3; R = CH_3, *n*-C_3H_7, *i*-C_3H_7) complexes in solution in methanol−water containing small amounts of nitric acid. Later the study was extended to the complete lanthanide series, using *i*-C_3H_7−BTP as the ligand.[18] These investigations approach more realistic conditions than in the single-crystal X-ray crystallography studies. Predominantly Eu·(BTP)$_3$ complexes were identified for the more hydrophobic propyl-BTPs. Conditional stability constants for the 1:3 complexes were calculated and found to increase approximately 4 orders of magnitude from lanthanum to lutetium. More recently, the conditional stability constant for the Eu·(*i*-C_3H_7−BTP)$_3$ complex has been determined from time-resolved laser-induced fluorescence spectroscopic (TRLFS) results,[19] which corroborate the previous finding.[17]

Theoretical, as well as experimental, studies of the selectivity of BTP as partitioning extractant have been published in the literature. In a theoretical study, Ionova et al.[20] offered an explanation for the low affinity of BTPs toward lanthanides. These authors deduce from quantum-chemical calculations that the nitrogen cavity of the BTP molecule is too small to comfortably sterically accommodate Ln(III) cations. Additionally, a positive charge of the central ring of the BTP molecule is said to repel the lanthanide cations. Gutierrez et al.[21] performed DFT calculations on the geometries of 1:1 complexes of selected lanthanides (La, Eu, Lu) with several N-donor ligands, among them H−BTP. Calculated structures are in fair to good agreement with published crystal structures.

(8) Nash, K. L. In *Handbook on the physics and chemistry of rare earths, Vol. 18*; Gschneidner, K. A., Jr., Eyring, L., Choppin, G. R., Lander, G. H., Eds.; Elsevier Science: Amsterdam, 1994.
(9) Drew, M. G. B.; Guillaneux, D.; Hudson, M. J.; Iveson, P. B.; Russell, M. L.; Madic, C. *Inorg. Chem. Commun.* **2001**, *4*, 12−15.
(10) Iveson, P. B.; Rivière, C.; Guillaneux, D.; Nierlich, M.; Thuéry, P.; Ephritikhine, M.; Madic, C. *Chem. Commun.* **2001**, 1512−1513.
(11) Seaborg, G. T. *Radiochim. Acta* **1993**, *61*, 115−122.
(12) Berthet, J. C.; Miquel, Y.; Iveson, P. B.; Nierlich, M.; Thuèry, P.; Madic, C.; Ephritikhine, M. *J. Chem. Soc., Dalton Trans.* **2002**, 3265−3272.
(13) Mazzanti, M.; Wietzke, R.; Latour, J.-M.; Pécaut, J.; Maldivi, P.; Remy, M. *Inorg. Chem.* **2002**, *41*, 2389−2399.
(14) Karmazin, L.; Mazzanti, M.; Bezombes, J.; Gateau, C.; Pécaut, J. *Inorg. Chem.* **2004**, *43*, 5147−5158.
(15) Wietzke, R.; Mazzanti, M.; Latour, J.-M.; Pécaut, J.; Cordier, P. Y.; Madic, C. *Inorg. Chem.* **1998**, *37*, 6690−6697.
(16) Karmazin, L.; Mazzanti, M.; Gateau, C.; Hill, C.; Pécaut, J. *Chem. Commun.* **2002**, 2892−2893.
(17) Colette, S.; Amekraz, B.; Madic, C.; Berthon, L.; Cote, G.; Moulin, C. *Inorg. Chem.* **2002**, *41*, 7031−7041.
(18) Colette, S.; Amekraz, B.; Madic, C.; Berthon, L.; Cote, G.; Moulin, C. *Inorg. Chem.* **2003**, *42*, 2215−2226.
(19) Colette, S.; Amekraz, B.; Madic, C.; Berthon, L.; Cote, G.; Moulin, C. *Inorg. Chem.* **2004**, *43*, 6745−6751.
(20) Ionova, G.; Rabbe, C.; Guillaumont, R.; Ionov, S.; Madic, C.; Krupa, J.-C.; Guillaneux, D. *New J. Chem.* **2002**, *26*, 234−242.
(21) Gutierrez, F.; Rabbe, C.; Poteau, R.; Daudey, J. P. *J. Phys. Chem. A* **2005**, *109*, 4325−4330.

In this study, we report results on the characterization of curium(III) and europium(III) complexation with *n*-C_3H_7−BTP using a combination of TRLFS and extended X-ray absorption fine-structure (EXAFS) spectroscopy. Quantum-chemical calculations are performed to complement the experimental investigations. The Cm^{3+} and Eu^{3+} aquo-ion species are also investigated as reference compounds. A number of features in this study are outstanding. First, the complexes are prepared under conditions as close as possible to actual partitioning conditions by extraction of metal nitrates from nitric acid into a solution of *n*-C_3H_7−BTP dissolved in a kerosene/octanol mixture. The experimental investigations are made on the extracted complexes in the separated organic phase. Second, for the first time curium is used as representative for the trivalent minor actinides relevant to the P&T strategy (which indeed are americium and curium). Third, the EXAFS data is evaluated using both conventional analysis methodology and a newly reported method of Monte Carlo simulation.[22,23] The Monte Carlo simulation allows us to model the three-dimensional structure of the complexes by using the experimental EXAFS spectra and the structure of the interacting ligand as constraints. Fourth, quantum-chemical calculations are performed on the whole molecule (i.e., Cm·$(BTP)_3$ and Eu·$(BTP)_3$).

Characterization of the complexes by means of TRLFS, EXAFS, and quantum-chemical calculations and the comparison of results for Cm(III) to those for Eu(III) should provide answers to the following open questions.

- Do we find a difference in Cm−N versus Eu−N bond lengths or differences in the complex structures, which might indicate a structural rationale for the selectivity of BTPs?
- Do the metal−ligand structures in organic solution agree with those reported for single crystals?
- Is there a difference in the complex stabilites of Cm·(*n*-C_3H_7−BTP)$_3$ and Eu·(*n*-C_3H_7−BTP)$_3$, which mirrors the Cm/Eu selectivity found for liquid−liquid extraction?
- Is U(III), used in previous studies by other authors, a useful surrogate for the target minor trivalent actinides to be separated (americium and curium)?

Experimental Section

Sample Preparation. *n*-C_3H_7−BTP is synthesized as described in ref 1. Metal complexes to be measured by EXAFS are prepared by extracting ^{248}Cm(III) or Eu(III) in 0.01 M HNO_3 and 2 M $NaNO_3$ into a solution of 0.04 M *n*-C_3H_7−BTP in TPH[24]/*n*-octan-1-ol (7:3 vol/vol). After the phases separated, the organic phase is transferred into sealed polyethylene vials for measurement. The metal-ion concentration in the organic phases is 5×10^{-3} M Cm(III) or Eu(III), resulting in a ligand-to-metal concentration ratio of 8.

For the Cm(III) titration experiments, 30 μL of a solution containing 6.05×10^{-6} M $CmCl_3$ is evaporated to dryness and dissolved in 1500 μL of TPH/*n*-octan-1-ol (7:3 vol/vol). Then, 750 μL of 1.51×10^{-4} M *n*-C_3H_7−BTP in TPH/*n*-octan-1-ol (7:3 vol/vol) is added in 10 375-μL portions, and the spectra are recorded after each addition. The ligand-to-curium concentration ratio ranges from 8.3 to 624. The Eu(III) titration is performed in a similar manner using 36 μL of a 5.0×10^{-4} M Eu stock solution and increasing additions of a 1.51×10^{-2} M *n*-C_3H_7−BTP solution. The ligand-to-europium concentration ratios range from 8.4 to 629. In addition, two reference samples are prepared containing 4×10^{-8} M Cm(III) or 5×10^{-5} M Eu(III), both in 0.03 M HCl.

XAFS Measurements. XAFS measurements are performed at Argonne National Laboratory (ANL) Advanced Photon Source (APS), with the electron-storage ring running under top-up mode with a 104 mA current, at the BESSRC beamline 12-BM. A pair of Si(111) crystals are used in the double-crystal monochromator. The Cm L3 edge spectra are calibrated by defining the first inflection point in the first derivative X-ray absorption near-edge structure (XANES) spectrum of a Zr foil, defined as 17.998 keV, which is recorded at the beginning of the Cm L3 EXAFS measurements and again at the end. No significant energy shift between the measurements is observed. The Eu L3 edge spectra are calibrated in a similar manner using an Fe foil as energy reference (7.112 keV). Sample vials are mounted in the Actinide Facility sample changer, and the spectra are recorded in fluorescence mode using a Canberra LEGe 13-element solid-state detector. Three to four scans are averaged, and the EXAFS is extracted using standard procedures and the WinXAS software.[25]

Conventional analysis of EXAFS data is made by performing theoretical least-squares fits of the EXAFS spectra to the EXAFS equation in *R* space using the feffit software.[26] Metric parameters describing the different coordination shells surrounding curium or europium are obtained: coordination numbers (*N*), interatomic distances (*R*), mean square radial displacements or EXAFS Debye−Waller factors (σ^2), and relative shifts in ionization potential (ΔE_0). All fitting operations to data of extracted complexes are performed to Fourier transform (FT) spectra in *R* space between 1.23 and 3.68 Å for the Cm L3 edge data for Cm complexed with *n*-C_3H_7−BTP and between 1.23 and 3.2 Å for the corresponding Eu data. EXAFS values are Fourier transformed in the *k* space shown using symmetric square windows with $\Delta k = 0.1$ Å^{-1} "Hanning sills". The amplitude reduction factor S_0^2 is held constant at 1 during fits. Theoretically calculated scattering phase-shift and backscattering amplitude functions are used in the fits. These are calculated with the ab initio multiple-scattering code feff8.[27] A cluster composed of 55 atoms (1 Cm atom and 54 C and N atoms from three BTP ligands, excluding rest groups on the triazine rings) with Cartesian coordinates for the Ce complex reported in ref 10 is used for the calculation. The EXCHANGE 3 2 1 control card in feff8 is specified (defines a Dirac−Hara local-density approximation for the real part of the photoelectron self-energy, a 2 eV real and 1 eV imaginary shift of the electron-gas estimated Fermi level), and muffin tins are automatically overlapped by default.

The FT data is initially fit to the EXAFS equation using a model of two coordination shells: one N and one composed of either N or C. Because these are $Z + 1$ elements, EXAFS cannot differentiate between them as backscattering nearest neighbors. Fits using N and those using C from the second shell both yielded essentially the same results. The results of these initial fits show three *n*-C_3H_7−BTP ligands to coordinate both Cm(III) and Eu(III). The data are then modeled using all C and N atoms of the BTP molecule (without the *n*-propyl rest groups on the triazine rings) and multiplied by three to account for coordination by three *n*-C_3H_7−BTP ligands.

(22) Rossberg, A.; Scheinost, A. C. *Phys. Scr.* **2005**, *T115*, 912−914.
(23) Rossberg, A.; Scheinost, A. C. *Anal. Bioanal. Chem.* **2005**, published on-line July 29, 2005.
(24) TPH is a French kerosene-type diluent. It was bought from Prochrom, France.
(25) Ressler, T. *J. Phys. IV* **1997**, *7-C2*, 269-270.
(26) Stern, E. A.; Newville, M.; Ravel, B.; Yacoby, Y.; Haskel, D. *Physica B* **1995**, *208−209*, 117−120.
(27) Ankudinov, A. L.; Ravel, B.; Rehr, J. J.; Conradson, S. D. *Phys. Rev. B* **1998**, *58*, 7565−7576.

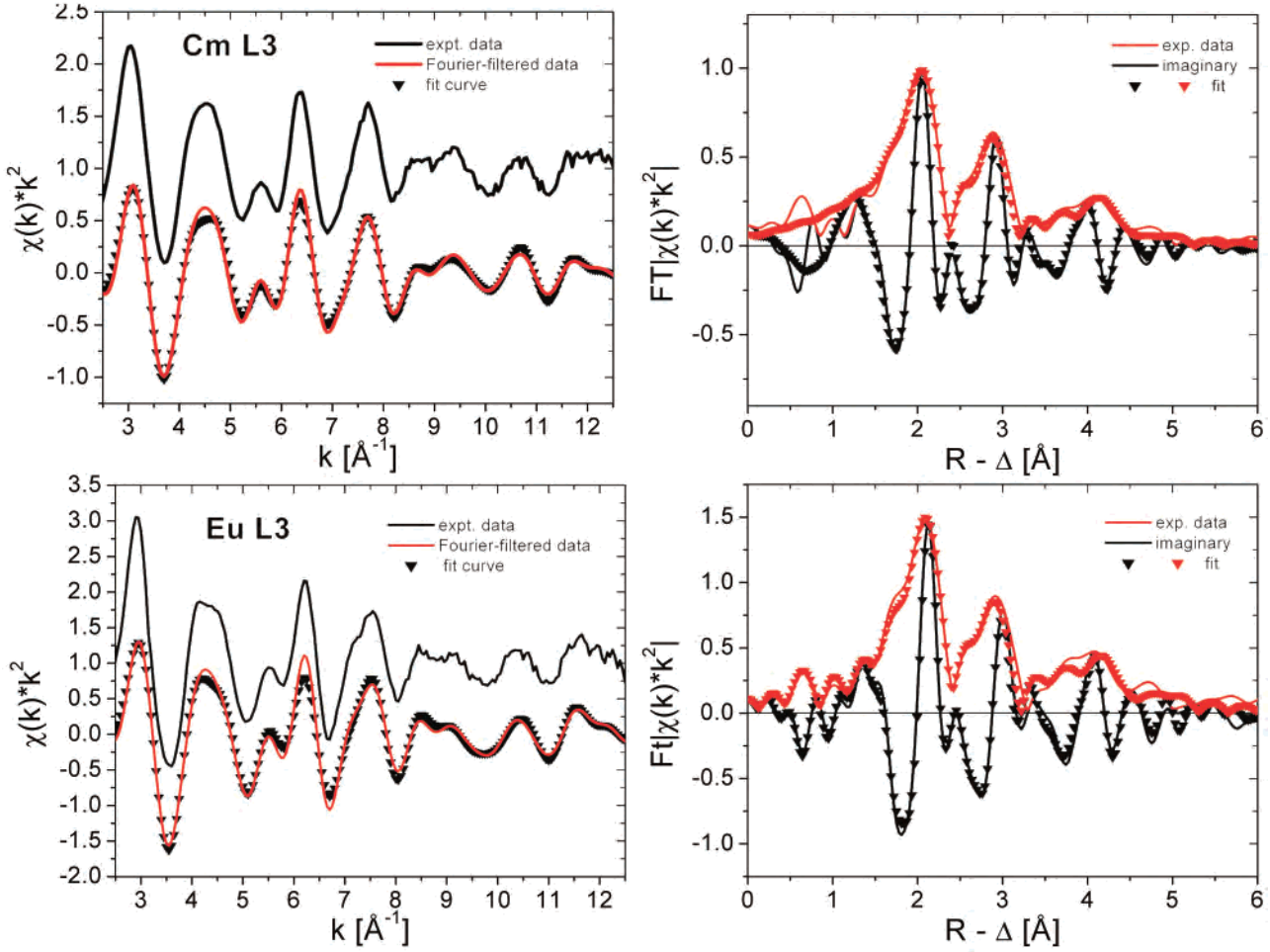

Figure 1. k^2 weighted L3 edge EXAFS (left) of Cm·(n-C_3H_7−BTP)$_3$ (top) and Eu·(n-C_3H_7−BTP)$_3$ (bottom) and their corresponding Fourier transform (FT) data (right).

The EXAFS data in this study is also analyzed using a recently reported Monte Carlo method. This Monte Carlo method is described in refs 22 and 23.

TRLFS Measurements. TRLFS measurements are performed using an excimer pumped-dye laser system (Lambda Physics, EMG 201 and FL 3002). A wavelength of 375.0 nm for Cm(III) and 394.0 nm for Eu(III) is used for excitation. Emission spectra are recorded from 580 to 630 nm after a constant delay time of 1.2 μs to discriminate short-lived organic fluorescence of the ligand. The fluorescence emission is detected by an optical multichannel analyzer consisting of a polychromator (Jobin Yvon, HR 320) with a 1200 lines/mm grating and an intensified photodiode array (Spectroscopy instruments, ST 180, IRY 700G). Details on the experimental setup are given elsewhere.[28]

Quantum-Chemical Calculations. Quantum-chemical calculations are carried out for M(III)·(H−BTP)$_3$, M(III)·(CH_3−BTP)$_3$, and M(III)·(terpy)$_3$ with M = La, Eu, Gd, Ac, and Cm, with the TURBOMOLE V5.7 software package[29] at different levels of theory.[30] The lanthanides are described using large-core effective-core potentials (ECP),[31] whereas the actinides are described with small-core ECPs and corresponding basis sets of the Stuttgart type.[32] The TZVP basis sets provided with TURBOMOLE are used for C, N, and H. For La, where TURBOMOLE provides basis sets of TZVP and TZVPP type, the basis set dependence of the La−N distances is investigated and found to be small (<0.01 Å), as is the change from H−BTP to CH_3−BTP. The effect of methyl groups on BTP is calculated for Eu(III) and found to be of the same, negligible order. For La·(H−BTP)$_3$, La·(CH_3−BTP)$_3$, and La·(terpy)$_3$, the structure is optimized at the RIDFT level with the BP functional and results in a D_3 symmetry. This symmetry is confirmed by analyzing the harmonic frequencies. This implies that the three N_{py} atoms as well as the six coordinating N_{tz} atoms in the three BTP molecules are equivalent. The calculations for the other metal ions are carried out with symmetry constrained to D_3 symmetry, as symmetry breaking because of the partially filled f shell is not expected.

Results and Discussion

XAFS Measurements. EXAFS spectra and theoretical fit curves are shown in Figure 1 for Cm(III) and Eu(III) complexed with n-C_3H_7−BTP. Metal complexes are prepared by extracting ^{248}Cm(III) or Eu(III) from acidic (HNO_3) aqueous solutions into an organic phase containing n-C_3H_7−

(28) Chung, K. H.; Klenze, R.; Park, K. K.; Paviet-Hartmann, P.; Kim, J. I. *Radiochim. Acta* **1998**, *82*, 215−219.
(29) Ahlrichs, R.; Bär, M.; Häser, M.; Horn, H.; Kölmel, C. *Chem. Phys. Lett.* **1989**, *162*, 165−169
(30) A detailed presentation of the quantum-chemical calculations, including technical details, is in preparation.
(31) Dolg, M.; Stoll, H.; Savin, A.; Preuss, H. *Theor. Chim. Acta* **1989**, *75*, 173-194.
(32) Kuechle, W. Diplomarbeit, Universität Stuttgart, Stuttgart, Germany, 1993.

Table 1. Metrical Parameters from Fits of Cm/Eu L3 Edge *R* Space Data in Figure 1[a]

sample	shell	N^b	R (Å)[c]	σ^2 (Å^2)[d]	ΔE_0 (eV)[e]	r factor[f]
Cm·(n-C_3H_7−BTP)$_3$	N	9	2.568 (0.007)	0.0051 (0.0007)	1.1 (0.8)	0.025
	C/N	18	3.431 (0.009)	0.005 (0.001)		
	C/N	18	4.81 (0.03)	0.004 (0.003)		
	C	9	5.30 (0.04)	0.001 (0.006)		
Eu·(n-C_3H_7−BTP)$_3$	N	9	2.559 (0.008)	0.0044 (0.0008)	2.5 (0.9)	0.028
	C/N	18	3.42 (0.01)	0.006 (0.001)		
	C/N	18	4.82 (0.02)	0.004 (0.003)		
	C	9	5.30 (0.03)	−0.002 (0.003)		
U·(n-C_3H_7−BTP)$_3$	N	9	2.54(7)			
Ce·(n-C_3H_7−BTP)$_3$	N	9	2.61(8)			
Sm·(n-C_3H_7−BTP)$_3$	N	9	2.57(8)			

[a] Estimated standard deviations are listed in parentheses and do not include systematic errors. S_0^2 is fixed at 1. For comparison, the average bond lengths for the first shell of coordinating N atoms from crystal structures of U, Ce,[10] and Sm[9] complexes are included. [b] Coordination numbers, held constant at given values. [c] Interatomic distances. [d] Debye−Waller factors. [e] Relative shifts in ionization potential. [f] Parameter describing goodness of fit = weighted sum of squares of residuals divided by the degree of freedom.

BTP, at a concentration relevant to liquid−liquid extraction.[4] The spectra of the two complexes are qualitatively similar.

Initial fits to the data using a model of two coordination shells reveal that the number of coordinating N atoms in the first shell is found to be ∼9 and two times as many C/N atoms (i.e., 18) are found in the second shell. This indicates three n-C_3H_7−BTP ligands are bound to both Cm(III) and Eu(III). For this reason, the data is modeled with four coordination shells, with 9 nearest N atoms directly bound to the metal cations, the second and third shells of 18 C/N atoms each (designated C/N and C′/N′, respectively), and a fourth, most distant shell of 9 C atoms, located para to N_{py} and N_{tz}, respectively (Scheme 1). Three significant three-legged multiple-scattering paths (Cm/Eu → N → C/N → Cm/Eu, Cm/Eu → C/N → C′/N′ → Cm/Eu, and Cm/Eu → N → C′/N′ → Cm/Eu) are included in the fits with their effective path lengths correlated to the single-scattering distances involved. Global ΔE_0 and σ^2 are also varied. The n-propyl groups of the triazine rings are not included. The results are listed in Table 1.

Note, we observe no evidence for coordinated nitrate groups in FTs of the fit residuals of backtransformed spectra. Bidentate-coordinated nitrate groups should show O atoms near 2.45−2.55 Å. The associated-nitrate N atom would be expected to be near 3 Å and the distal O atom near 4.2 Å. Especially, the 3 Å nitrate N atom distance is not observed, and this distance does not coincide with the C/N distances to Cm(III) or Eu(III) in the complexes (Table 1). We conclude that neither the Cm(III) nor the Eu(III) complex have nitrate (formally required for charge neutralization) directly coordinated. Figure 2 shows the structure of the complex.

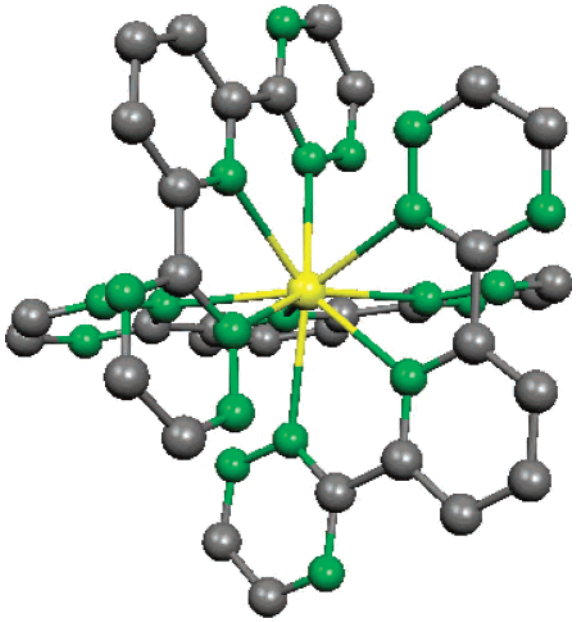

Figure 2. Structure of the Cm/Eu·(n-C_3H_7−BTP)$_3$ complex (green = N, gray = C, yellow = metal; the H atoms and n-propyl groups not shown).

A comparison of results in Table 1 shows that those for Cm are not significantly different than those for Eu, indicating that the coordination structure of Cm·(n-C_3H_7−BTP)$_3$ and Eu·(n-C_3H_7−BTP)$_3$ are the same. The observed selectivity of n-C_3H_7−BTP for Cm(III) over Eu(III) is not structural in origin; the metal cation complexes coordinated with three ligands have the same coordination structure.

Comparing our data with literature data for crystalline compounds,[9,10] we find good agreement. However, in contrast to the differences in interatomic distances reported for U·(n-C_3H_7−BTP)$_3$ versus Ce·(n-C_3H_7−BTP)$_3$,[10] we observe no difference in the metrical parameters of Cm·(n-C_3H_7−BTP)$_3$ and Eu·(n-C_3H_7−BTP)$_3$. This can be compared to EXAFS results from Jensen et al.,[33] who report no significant differences in bond lengths for Cm(III), Sm(III), and Nd(III) complexed with bis(2,4,4-trimethylpentyl)dithiophosphinic acid, an extractant with an exceptional selectivity for An(III) over Ln(III).[34] Similar results have also been reported for Am(III)[35] versus La(III), Nd(III), and Eu(III).[36] Den Auwer et al.[37] found the structures of Am(III) and Nd(III) complexed with N,N,N′,N′-tertamethylmalonamide

(33) Jensen, M. P.; Bond, A. H. *J. Am. Chem. Soc.* **2002**, *124*, 9870−9877.
(34) Zhu, Y.; Chen, J.; Jiao, R. *Solvent Extr. Ion Exch.* **1996**, *14* (1), 61−68.
(35) Tian, G.; Zhu, Y.; Xu, J.; Hu, T.; Xie, Y. *J. Alloys Compd.* **2002**, *334*, 86−91.
(36) Tian, G.; Zhu, Y.; Xu, J.; Zhang, P. *Inorg. Chem.* **2003**, *42*, 735−741.

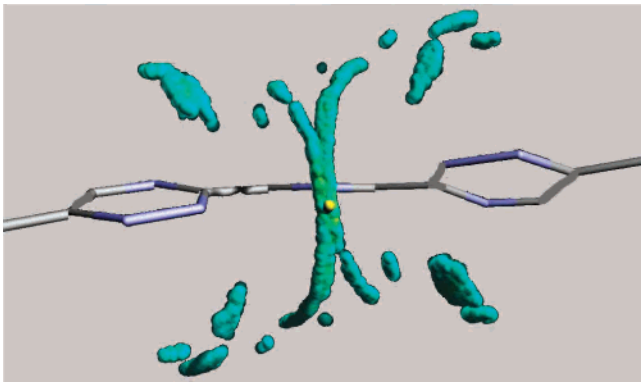

Figure 3. Standard deviation (STD) between experimental spectra and theoretically calculated EXAFS for random positions of Cm(III) relative to the BTP molecule shown (see text for details). Yellow designates the position with the smallest STD or the most probable position. Blue designates large STD or least probable positions (Cm positions with a STD > 1.55 are not shown). The BTP's central pyridine ring in this picture lies normal to the plane projection and the two lateral triazine rings are twisted at a 10−15° dihedral angle.

(TEMA) to be similar when compared using EXAFS. However, TEMA bonds via oxygen atoms and shows no selectivity for Am(III) over Nd(III). In contrast, significant structural differences are found[38] for Cm(III) and Eu(III) complexed with a synergistic mixture of di(chlorophenyl)-dithiophosphinic acid and tri-*n*-octylphosphine oxide, a system with a high selectivity for An(III) over Ln(III).[39]

The input parameters for the Monte Carlo simulation are the ligand structure of BTP molecule (taken from ref 10), approximate values for σ^2 of O and N atoms (both 0.004 Å^2), and ΔE_0 determined by conventional EXAFS shell fitting. Using these parameters and the parametrized EXAFS equation for random positions of a Cm atom at the BTP molecule, we calculate theoretical EXAFS spectra. It is assumed that each of the three BTP molecules is coordinated identically to the Cm atom. Therefore, the Cm atom is randomly moved in a defined 10 Å diameter sphere relative to one BTP molecule, and the scattering contributions of the ligand atoms to the calculated EXAFS are multiplied by a factor of 3. The center of the 10 Å diameter sphere is positioned at the N_{py}. During the MC simulation, the Cm atom is positioned randomly at around one million random positions in the sphere, and the corresponding theoretical calculated EXAFS spectra are compared with the experimental EXAFS spectrum. The standard deviations (STD) between the theoretical EXAFS spectra and the experimental EXAFS spectrum are shown for random Cm positions in Figure 3, excluding STD > 1.55. The yellow sphere in Figure 3 designates the best agreement between the theoretical and experimental spectra (STD = 0.96) achieved and therefore defines the true Cm position relative to the BTP ligand.

The Cm−N bond distances determined by our MC approach are 2.59 and 2.57 Å (N_{tz}) and 2.52 Å (N_{py}). The resulting average for the three Cm−N bond distances of 2.56 Å is in good agreement with the Cm−N bond distance determined by conventional shell fitting (Table 1). The splitting of the Cm−N distances may result from the BTP ligand structure, which is fixed during the MC simulation as shown in Figure 3.

TRLFS Measurements. Figure 4 shows the fluorescence spectra of Cm(III) and Eu(III) in the presence of increasing amounts of *n*-C_3H_7−BTP in TPH/*n*-octan-1-ol. For Cm(III), exclusively one species is formed, independent of the ligand-to-metal ratio, which is increased from 8.3 to 624. EXAFS results, which are obtained with a ligand-to-metal ratio of 8, identifies this species as Cm·(*n*-C_3H_7−BTP)$_3$. The formation of Cm·(*n*-C_3H_7−BTP) and Cm·(*n*-C_3H_7−BTP)$_2$ is not observed in the concentration range examined.

The emission spectra of the Cm·(*n*-C_3H_7−BTP)$_3$ complex formed during titration is compared to that of the Cm^{3+} aquo ion in Figure 4a. The fluorescence spectrum of Cm·(*n*-C_3H_7−BTP)$_3$ displays an emission band at 613.0 nm with a distinct shoulder at the blue flank of the spectrum, which is the result of a strong ligand-field splitting (i.e., a strong ligand−metal interaction). In comparison to that of the Cm^{3+} aquo ion, the spectrum of Cm·(*n*-C_3H_7−BTP)$_3$ is shifted 19.3 nm to higher wavelength. This bathochromic shift is a result of the strong interaction between the three *n*-C_3H_7−BTP ligands and the Cm(III) cation.

The spectral evolution of the fluorescence spectra resulting from $^5D_0 \rightarrow {}^7F_2$ and $^5D_0 \rightarrow {}^7F_1$ transitions as a function of the ligand concentration is shown in Figure 4b and compared to the spectrum of the Eu^{3+} aquo ion. Contrary to the Cm(III) data, the Eu(III) emission spectra are observed to change during the titration; at least two different Eu·(*n*-C_3H_7−BTP)$_x$ species are formed for ligand-to-metal concentration ratios ranging from 8.3 to 629. In addition, changes in the Eu(III) coordination sphere cause only small shifts of the fluorescence peak wavelength. Compared to that of the Eu^{3+} aquo ion, the coordination with *n*-C_3H_7−BTP causes a distinct splitting of the $^5D_0 \rightarrow {}^7F_1$ emission band. The fluorescence peak of the $^5D_0 \rightarrow {}^7F_2$ transition is shifted from 615.9 nm ([L]/[M] = 8.4) to 617.7 nm ([L]/[M] = 629) during the titration. The $^5D_0 \rightarrow {}^7F_2$ transition is hypersensitive and changes in the ligand field of Eu(III) are reflected by changes of the transition ratio ($^7F_2/^7F_1$). Whereas the Eu^{3+} aquo ion displays a transition ratio $^7F_2/^7F_1 < 0.6$, the ratio increases to 1.16 for [L]/[M] = 8.4 and decreases again to 1.06 ([L]/[M] = 629) with increasing ligand concentration.

A comparison with reports in the literature shows that the Eu·(*i*-C_3H_7−BTP)$_3$ fluorescence spectrum measured in methanol/water (1:1 vol/vol)[19] is identical to our Eu·(*n*-C_3H_7−BTP)$_x$ fluorescence spectra in TPH/*n*-octan-1-ol (7:3 vol/vol) at high ligand-to-metal concentration ratios. This means that Eu·(*n*-C_3H_7−BTP)$_3$ is exclusively formed only at ligand-to-metal concentrations ratios >300, for the concentrations studied. The fact that EXAFS results identify Eu·(*n*-C_3H_7−BTP)$_3$ at a ligand-to-metal concentration ratio of 8 may appear surprising; however, EXAFS samples are prepared at total ligand concentrations more than two (Eu) and four (Cm) orders of magnitude higher than are the TRLFS study

(37) Den Auwer, C.; Charbonnel, M. C.; Drew, M. G. B.; Grigoriev, M.; Hudson, M. J.; Iveson, P. B.; Madic, C.; Nierlich, M.; Presson, M. T.; Revel, R.; Russell, M. L.; Thuéry, P. *Inorg. Chem.* **2000**, *39*, 1487−1495.
(38) Weigl, M.; Denecke, M. A.; Panak, P. J.; Geist, A.; Gompper, K. *Dalton Trans.* **2005**, 1281−1286.
(39) Modolo, G.; Odoj, R. *Solvent Extr. Ion Exch.* **1999**, *17* (1), 33−53.

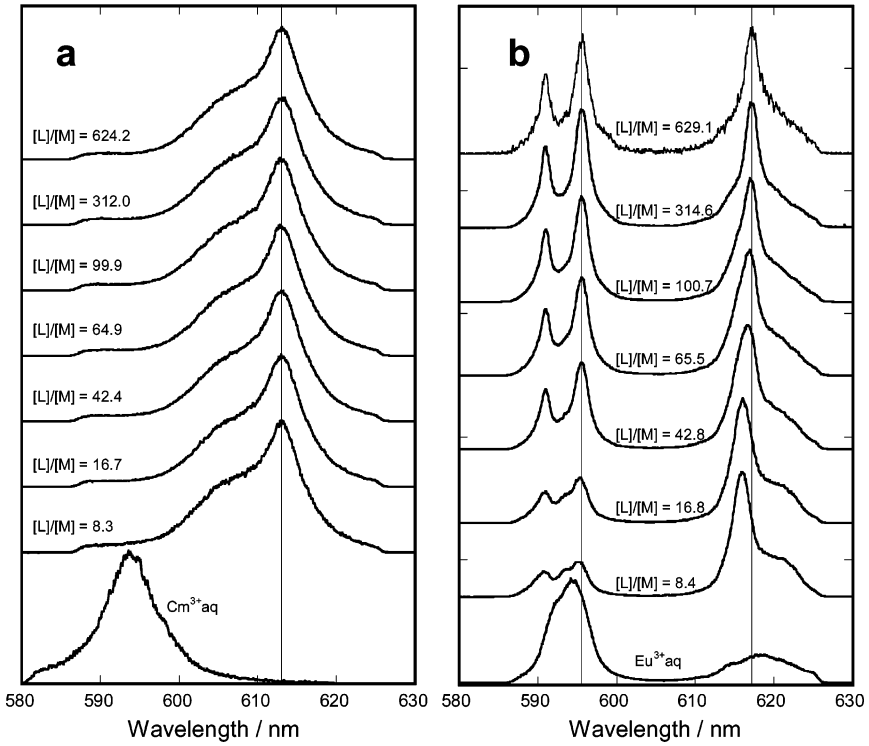

Figure 4. Fluorescence spectra of Cm(III) (a) and Eu(III) (b) as a function of the ligand-to-metal concentration ratios indicated.

Table 2. Optimized M−N Distances to Pyridine N ($M-N_{Py}$) and Triazinyl N2 ($M-N_{tz}$)[a]

functional/ method[30]	Cm		Eu	
	$M-N_{py}$ (Å)	$M-N_{tz}$ (Å)	$M-N_{py}$ (Å)	$M-N_{tz}$ (Å)
B3-LYP	2.646	2.636	2.640	2.633
BH-LYP	2.633	2.622	2.621	2.614
B-LYP	2.667	2.654	2.661	2.654
B−P	2.614	2.616	2.618	2.623
TPSS	2.607	2.606	2.614	2.616
RI-MP2	−	−	2.549	2.556

[a] All calculations are carried out with symmetry restrictions to the D_3 point group.

samples. This obviously pushes the equilibrium to favor formation of Eu·(*n*-C_3H_7−BTP)$_3$.

These results prove that Cm·(*n*-C_3H_7−BTP)$_3$ is formed at much lower ligand-to-metal concentration ratio, which is in accordance with the higher affinity of *n*-C_3H_7−BTP toward An(III) and consistent with its selectivity in liquid−liquid extraction.[4] Similar results were found when the complexation of U(III) was compared to that of Ce(III) using Me-BTP.[10]

Quantum-Chemical Calculations. The following interpretation of our quantum-chemical calculation focuses on the comparison of the M−N bond distances for the Cm·(BTP)$_3$ and Eu·(BTP)$_3$ complexes and some energetic trends in their relative binding energies.

DFT calculations, unrestricted in the case of Cm(III), are carried out with several functionals available in TURBOMOLE. Calculated M−N bond lengths are compiled in Table 2. For most of the functionals used, the differences in M−N distances within a given complex and the differences between Cm·(BTP)$_3$ and Eu·(BTP)$_3$ are on the order of 0.01 Å, although the averaged distances scatter. The calculations do not give a clear indication which of the two symmetry-distinct M−N bonds is the shorter one. The BTP ligand in all calculations is nearly planar, with a low-frequency torsion mode found for the La·BTP$_3$ complex.

In agreement with the experiments, we conclude that DFT gives the same metal−ligand bond distances to BTP for Cm(III) and Eu(III), within acceptable error. As the absolute bond distances scatter, depending on the choice of the functional, Eu·(BTP)$_3$ is additionally optimized at the RI-MP2 level, correlating the 5s, 5p shells on Eu(III) and all electrons of the ligand, except the 1s electrons of C and N. An average Eu−N bond distance of 2.554 Å is found, which is in excellent agreement with our EXAFS data (Table 1). The same good quantitative agreement between theory and experiment is found by comparing RI-MP2 calculations for La·(Me-BTP)$_3$ with crystal data.[12] Although our calculations have not yet converged at the RI-MP2-level for the Cm(III) complex, we conclude by combining results obtained at different levels of theory and the basis set tests, as well as the estimate of the effect of methyl groups, that the Cm−N and Eu−N bond distances are practically identical and in full agreement with the experimental data.

A theoretical explanation for the observed different extraction behavior of BTP for An(III) and Ln(III) is less straightforward, as the corresponding differences in binding energy are close if not below the possible calculation accuracy. To eliminate systematic errors and thermodynamic contributions, the relative binding energies of the exchange reaction

$$\mathrm{Eu{\cdot}(BTP)_3 + Cm{\cdot}(terpy)_3 \rightleftarrows Eu{\cdot}(terpy)_3 + Cm{\cdot}(BTP)_3}$$

are compared at the BP-DFT level. A preference for

$Cm\cdot(BTP)_3$ by only 3 kJ/mol is obtained. Although this result will change when refining the calculations, it is evident and in agreement with the experiment that the differences in binding energy relevant for the extraction process are small. A detailed bond analysis for these complexes at various levels of theory is planned to explore the differences between An(III) and Ln(III).

Conclusions

EXAFS results show Cm(III) and Eu(III) complexed with *n*-C_3H_7−BTP to have identical solution coordination structures. This finding is supported by the quantum-chemical calculations. This is in contrast to reported XRD structure analyses, which find U(III)−N bonds to be 0.06−0.09 Å shorter than the Ce(III)−N bonds in crystalline BTP complexes of these cations.[10] Similar trends are also reported for U(III) and Ln(III) complexed with tpza, tpzcn, and tpztn.[13,14] These contrasting results suggest that U(III) is not a suitable surrogate for Am(III) and Cm(III) when investigating An(III) versus Ln(III) selectivities of partitioning agents.

Whereas structural investigations by means of EXAFS reveal no significant differences in the coordination numbers and bond distances of $Cm\cdot(n\text{-}C_3H_7\text{−}BTP)_3$ and $Eu\cdot(n\text{-}C_3H_7\text{−}BTP)_3$, speciation studies by TRLFS reveal a different thermodynamic stability of the Cm(III) and Eu(III) complexes with *n*-C_3H_7−BTP. $Cm\cdot(n\text{-}C_3H_7\text{−}BTP)_3$ is exclusively formed for all ligand-to-metal concentration ratios investigated (>8), while a significantly higher ratio (>300) is needed to exclusively form the corresponding $Eu\cdot(n\text{-}C_3H_7\text{−}BTP)_3$ complex. These results are in good agreement with the selectivity of *n*-C_3H_7−BTP in a liquid−liquid extraction.[4] Together the EXAFS data, quantum-chemical calculations, and TRLFS results show that the *n*-C_3H_7−BTP selectivity for Cm(III) over Eu(III) is associated with a higher affinity of the ligand for An(III). Selectivity is related to a higher thermodynamic stability of $Cm\cdot(n\text{-}C_3H_7\text{−}BTP)_3$ and is not related to simple structural differences between complexes of An(III) and Ln(III), as there is no substantial difference between coordination structure of $Cm\cdot(n\text{-}C_3H_7\text{−}BTP)_3$ and $Eu\cdot(n\text{-}C_3H_7\text{−}BTP)_3$.

Acknowledgment. We are grateful for beamtime allocation at the BESSRC 12-BM station, support by the BESSRC beamline staff, and for experimental assistance and use of the infrastructure of the Actinide Facility. Use of the APS is supported by the U.S. Department of Energy, Office of Science, Office of Basic Energy Sciences, under Contract No. W-31-109-ENG-38. Furthermore, financial support from the Commission of the European Community is acknowledged (Contract FI6W-CT-2003-508854).

IC0511726